

THE CORRELATION BETWEEN STRUCTURAL RELAXATION PROCESS AND THE CHANGE IN MAGNETIC PERMEABILITY OF THE $\text{Fe}_{73.5}\text{Cu}_1\text{Nb}_3\text{Si}_{15.5}\text{B}_7$ AMORPHOUS ALLOY UNDER THE THERMAL INFLUENCE

Aleksandra Kalezić-Glišović*, Nebojša Mitrović, Aleksa Maričić

*University of Kragujevac, Faculty of Technical Sciences Čačak,
Joint Laboratory for Advanced Materials of SASA, Section for Amorphous Materials,
Svetog Save 65, 32000 Čačak, Republic of Serbia*

*Corresponding author; E-mail: aleksandra.kalezic@ftn.kg.ac.rs

(Received June 29, 2016; Accepted August 29, 2016)

ABSTRACT. Fast cooling of 10^6 K/s, according to the melt-spinning method, led to the $\text{Fe}_{73.5}\text{Cu}_1\text{Nb}_3\text{Si}_{15.5}\text{B}_7$ amorphous alloy formation. X-ray diffraction analysis method (XRD) showed that the obtained alloy is in amorphous state. The differential scanning calorimetry method (DSC) has defined the temperature interval of the crystallization process to be from 510°C to 540°C . The same temperature interval has also been confirmed by measuring electrical resistivity dependence over temperature. The heating of alloy sample in the temperature interval from 25°C to 600°C , leads to structural changes in the alloy under the thermal influence. Structural relaxation and crystallization processes have been investigated by thermoelectromotive force measurement (TEMF) of thermocouple amorphous alloy – copper. Based on the change in temperature coefficient of TEMF thermocouple annealed at various temperatures, relative changes in electron state density near Fermi level have been determined. It has been shown that the changes in normalized magnetic permeability in correlation with appropriate structural changes, which cause changes in electron state density near Fermi level.

Key words: thermoelectromotive force, electron state density near Fermi level, electrical resistivity, magnetic permeability.

INTRODUCTION

Amorphous metallic alloys (AMA) represent one of the classes of new materials, which thanks to their extraordinary properties have become applicable in almost all branches of technology, especially in electrical engineering (BERNAL, 1960; TAKAYAMA, 1976). It is a group of amorphous materials most oftenly obtained through quenching of the melts obtained by means of alloying of transitive metals (TM: Fe, Ni, Co, Ti, Mo, Nb, V, Cr, Zr, Pd), which possess magnetic and electrical properties, with metalloids (M: B, Si, P, C, Ge) which are supposed to slow down the crystallization process during the solidification of the melts. Large quenching rates of around 10^6 - 10^8 K/s enable atomic order not higher than 1 nm in the structure formed in this way (JONG *et al.*, 2005; SANTOS and SANTOS, 2001).

The amorphous state of the metallic glasses is, however, structurally and thermodynamically unstable and very susceptible to partial or complete crystallization during thermal treatment, which requires the knowledge of alloys stability in a wide range of temperatures. Generally, the stability is a thermally activated process of transition from disordered amorphous structure to an ordered crystal structure. The synthesis of amorphous soft magnetic alloys, obtained through melt quenching technique requires proper composition of the alloy. This ensures improved levels of the properties, such as a high glass-forming ability, good casting properties of the alloy which in turn determines the surface quality and uniformity of the melt-spun ribbons, as well as an enhanced thermal stability of both magnetic properties and amorphous structure (RAVAL, *et al.*, 2005; MARIČIĆ, *et al.*, 2008; MINIĆ *et al.*, 2009a). The researches show that magnetic properties after the crystallization process are weakened or improved provided nanocrystal phases are formed (HENDERSON, 1979; MATUSITA and SAKKA, 1980; MINIĆ *et al.*, 2009b).

Intensive researches on kinetic features of amorphous alloys show correlation between the physical nature of the anomalous behavior of electron state density near Fermi level, thermal conductivity, heat capacity and resistivity on the one hand and structural inhomogeneities in these materials on the other (RIBIĆ-ZELENOVIĆ *et al.*, 2008; KALEZIĆ-GLIŠOVIĆ, 2012; MARIČIĆ *et al.*, 2012]. At temperatures of up to 100°C lower than the crystallization temperature, two competitive processes take place during annealing of amorphous alloys: on the one hand, free volume decreases, which lowers the rate of diffusion mass transport, and on the other hand, arranging processes bring the alloy closer to the crystallized state.

This paper aims to investigate effects of structural changes of amorphous alloy $\text{Fe}_{73.5}\text{Cu}_1\text{Nb}_3\text{Si}_{15.5}\text{B}_7$ during the annealing process on its magnetic permeability and thermoelectromotive force of the thermocouple amorphous alloy $\text{Fe}_{73.5}\text{Cu}_1\text{Nb}_3\text{Si}_{15.5}\text{B}_7 - \text{Cu}$ and to define the correlation among the structural changes, magnetic properties and TEMF change.

EXPERIMENTAL

The subject of the research this paper examines is ribbon-shaped AMA $\text{Fe}_{73.5}\text{Cu}_1\text{Nb}_3\text{Si}_{15.5}\text{B}_7$. The investigated ribbon samples were 30 μm thick and 70 mm length. Differential scanning calorimetry (DSC) measurement was performed using Netzsch DSC-404, in an argon atmosphere, at a heating rate of 20°C/min. Electrical resistivity of the amorphous ribbon was measured using 4-point method, in the oven under hydrogen atmosphere, to prevent oxidation during heating. Resistivity was measured non-isothermally during heating from 25°C to 650°C. By measuring TEMF during the multiple heatings of the thermocouple obtained by joining AMA and copper conductor, the changes in electron state density near Fermi level have been determined upon every annealing within 10 minutes. TEMF was measured by compensation method of $5 \cdot 10^{-6}$ V sensitivity. Modified Faraday method was used to investigate the temperature dependence of change in normalized magnetic permeability, in temperature range from room temperature up to 600°C, in argon atmosphere, at applied magnetic field of 8 kA/m. The heating run was 10°C/min.

RESULTS AND DISCUSSION

In our earlier paper (MARIČIĆ *et al.*, 2012) the results of thermal and thermoelectric measurements were shown for this alloy. Fig. 1 shows temperature dependence of electrical resistivity and DSC thermogram of the AMA $\text{Fe}_{73.5}\text{Cu}_1\text{Nb}_3\text{Si}_{15.5}\text{B}_7$ (MARIČIĆ *et al.*, 2012).

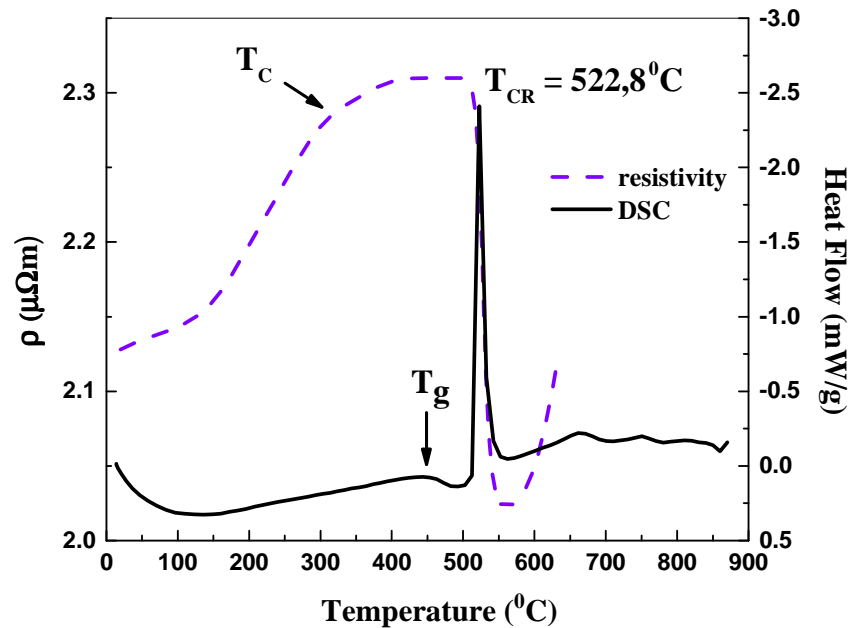


Figure 1. The temperature dependence of electrical resistivity and DSC thermogram (heating rate of 20 °C/min) of the $\text{Fe}_{73.5}\text{Cu}_1\text{Nb}_3\text{Si}_{15.5}\text{B}_7$ alloy sample (T_g – glass transition temperature, T_{CR} – crystallization temperature, T_C – Curie temperature).

The presented temperature dependence of electrical resistivity of as-cast alloy shows all the structural changes that occur within the investigated temperature interval. DSC thermogram shows that the temperature range before the crystallization from 150°C to 520°C can be split into structural relaxation region (150°C–440°C) and supercooled liquid region, which is in correlation with the measurement results $\rho(T)$. First within 150°C and 400°C the electrical resistivity increases, whereby two regions can be noticed (Fig. 1) in which the speed of the change in electrical resistivity varies, which is characteristic of metals. Then comes the region of almost constant resistivity (400°C–500°C), which corresponds to the supercooled liquid region. The biggest decrease in electrical resistivity occurs in the range of temperature crystallization, because the crystallization process is followed by the changes in electronic structure and the increase in the number of free electrons due to reduced number of covalent bonds, as well as the increased electron mean free path in the crystal state. Within the temperature interval of 520°C–630°C, the electrical resistivity starts to grow again. The presence of newly formed phases Fe_3Si and FeCu_4 (KALEZIĆ-GLIŠOVIĆ, 2012) in the amorphous matrix causes sudden increase in electrical resistivity at higher temperatures.

Thermomagnetic measurements were used to investigate the effect of structural relaxation process and crystallization process on magnetic properties of this alloy (Fig. 2). Upon a number of successive annealings of the same sample with gradually higher annealing temperature, magnetic permeability has increased by up to 40%. Normalized values of the magnetic permeability ($\mu_t^i/\mu_{20^\circ\text{C}}$) were obtained from the relation of magnetic permeability of the cooled sample upon every annealing ($i = 1, \dots, 6$) and magnetic permeability of the as-cast sample before heating ($\mu_{20^\circ\text{C}}$).

Upon first heating in the temperature range of amorphous state and upon cooling to room temperature, magnetic permeability increases by 7%. Upon second heating of up to 300°C, in temperature range of amorphous state and upon cooling to room temperature permeability rises by 35%, whereas after the third heating of up to 400°C it increases by 40%.

Upon the fourth annealing at 450°C it comes to a slight decline in magnetic permeability of the cooled sample for around 2% as compared to the permeability before the heating. The annealing of the sample at 550°C (above the crystallization temperature) leads to a significant fall in magnetic permeability of the cooled sample for around 60% as compared to the maximum permeability of the sample with relaxed amorphous structure, which was obtained upon annealing at 400°C. The increase in magnetic permeability upon each heating is caused by structural relaxation process. This process leads to a decrease in the density of defects, mechanical microstrains and free volume in the alloy sample, which enables greater mobility of magnetic domain walls. Furthermore, under the influence of thermal energy, the iron atoms with larger potential energy pass over the energy barriers and reach lower energy states. At these lower levels their 3d and 4s orbits better overlap with neighbouring atoms orbits, which causes the increased exchange interaction and increase in magnetic permeability. With simultaneous thermal treatment and the effect of external magnetic field, the disoriented in-between domain walls atoms assimilate with energetically more favourable domain. Upon cooling, this causes increase in magnetic permeability of the sample with relaxed amorphous structure. The fall in magnetic permeability of the cooled sample upon annealing at the temperature of 550°C was caused by the crystallization process of amorphous phase. The alloy sample with the crystal structure has significantly increased thermal stability of the structure. Now the alloy atoms are positioned with minimum potential energy, whereby the change in direction of the chaotically oriented magnetic domains in the applied magnetic field is harder, which causes the decline in magnetic permeability. Simultaneously, the increased thermal stability of the structure causes the increase in Curie temperature T_C of alloy with the crystal structure. Curie temperature T_C gets slightly higher upon every new annealing. This is caused by increase in thermal stability of the structure through structural relaxation process. Therefore, greater thermal energy for disorientation of magnetic domains is required. Curie temperature T_C of the sample with amorphous structure is in the temperature range from around 330°C to 370°C, which perfectly correlates with the results obtained through measurements of electrical resistivity (Fig. 1).

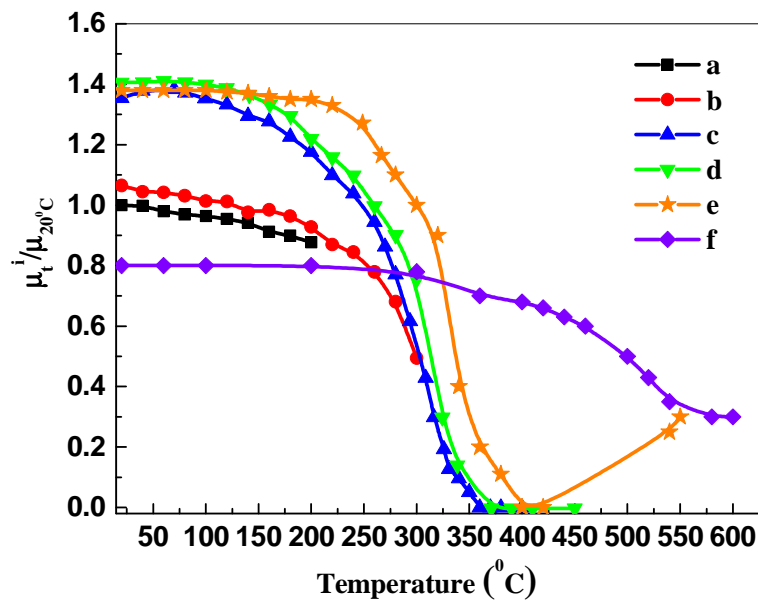


Figure 2. The temperature dependence of change in normalized magnetic permeability of AMA $\text{Fe}_{73.5}\text{Cu}_1\text{Nb}_3\text{Si}_{15.5}\text{B}_7$: a) first heating up to 200°C ($i=1$), b) second heating up to 300°C ($i=2$), c) third heating up to 400°C ($i=3$), d) fourth heating up to 450°C ($i=4$), e) fifth heating up to 550°C ($i=5$) and f) sixth heating up to 600°C ($i=6$) in argon.

The structural changes that occur during the structural relaxation process and crystallization process have been investigated by means of measurement of thermoelectromotive force of the thermocouple obtained through mechanical coupling of copper conductor (Cu) and tested AMA during multiple heatings of the same sample up to temperatures of $t_1 = 200^\circ\text{C}$, $t_2 = 300^\circ\text{C}$, $t_3 = 400^\circ\text{C}$, $t_4 = 450^\circ\text{C}$, $t_5 = 550^\circ\text{C}$ and $t_6 = 600^\circ\text{C}$ successively. The results of the measurements are shown in Fig. 3.

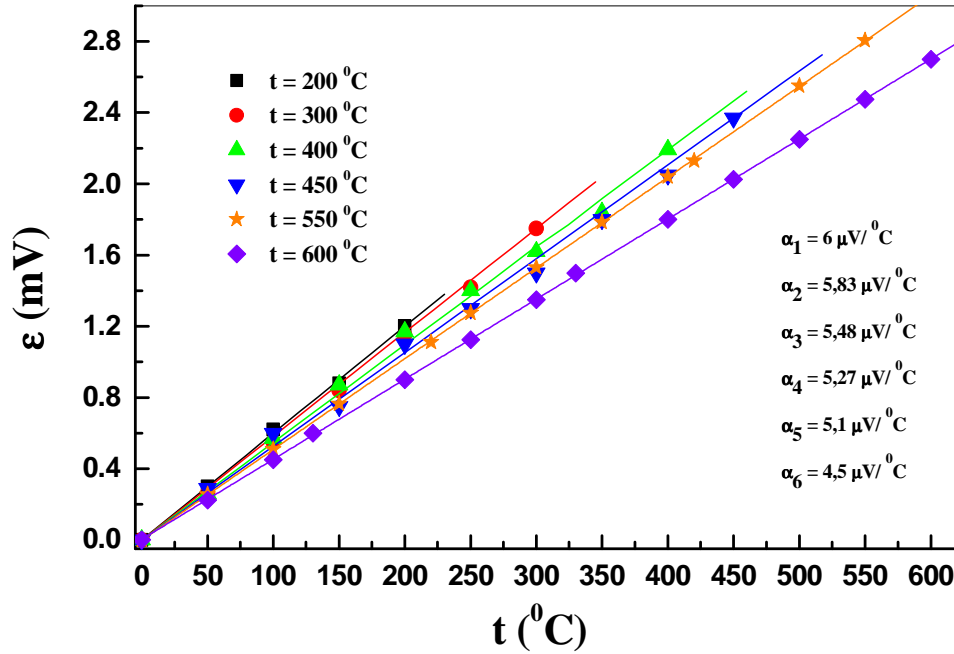


Figure 3. Thermoelectromotive force temperature dependence of the same sample of AMA $\text{Fe}_{73.5}\text{Cu}_1\text{Nb}_3\text{Si}_{15.5}\text{B}_7$ during multiple heatings of up to temperatures $t_1 = 200^\circ\text{C}$, $t_2 = 300^\circ\text{C}$, $t_3 = 400^\circ\text{C}$, $t_4 = 450^\circ\text{C}$, $t_5 = 550^\circ\text{C}$ and $t_6 = 600^\circ\text{C}$.

It has been shown that upon each heating there is a change in Seebeck coefficient α (Fig. 3), which represents the difference function of electron state density $n(E_F)$ near Fermi level as per the following relation:

$$\alpha = \frac{k}{2e} \left(\frac{n_1}{n_2} - \frac{n_2}{n_1} \right), \quad (1)$$

where e is electron charge, k is the Boltzmann's constant, n_1 is the electron state density near Fermi level in copper and n_2 is the electron state density near Fermi level in amorphous annealed alloy. With the increase in the annealing temperature the TEMF coefficient, i.e. Seebeck coefficient α decreases. Assuming that the electron state density in copper does not change during the heating, it is obvious that the change α is caused only by the change in electron state density in amorphous part of the thermocouple (RIBIĆ-ZELENOVIĆ *et al.*, 2008; MARIĆIĆ *et al.*, 2012; MINIĆ, *et al.*, 2009c).

Based on the slopes of the lines, according to the relation for the Seebeck effect $\varepsilon = \alpha \Delta T$, (ΔT – the difference in temperatures of two junctions), relative change in the electron state density near Fermi level has been determined in the amorphous part of the thermocouple upon each annealing

within 10 minutes: $\frac{\Delta n'_{2,1}}{n_{2,1}} = 2,83\%$, $\frac{\Delta n'_{2,2}}{n_{2,1}} = 8,67\%$, $\frac{\Delta n'_{2,3}}{n_{2,1}} = 12,17\%$, $\frac{\Delta n'_{2,4}}{n_{2,1}} = 15\%$ i $\frac{\Delta n'_{2,5}}{n_{2,1}} = 25\%$

(MARIČIĆ *et al.*, 2012) (Fig. 4a).

The diagram on Fig. 4 shows the dependance of the relative change in the electron state density near Fermi level, and the change in normalized values of magnetic permeability, over the annealing temperature of the cooled alloy sample $\text{Fe}_{73,5}\text{Cu}_1\text{Nb}_3\text{Si}_{15,5}\text{B}_7$.

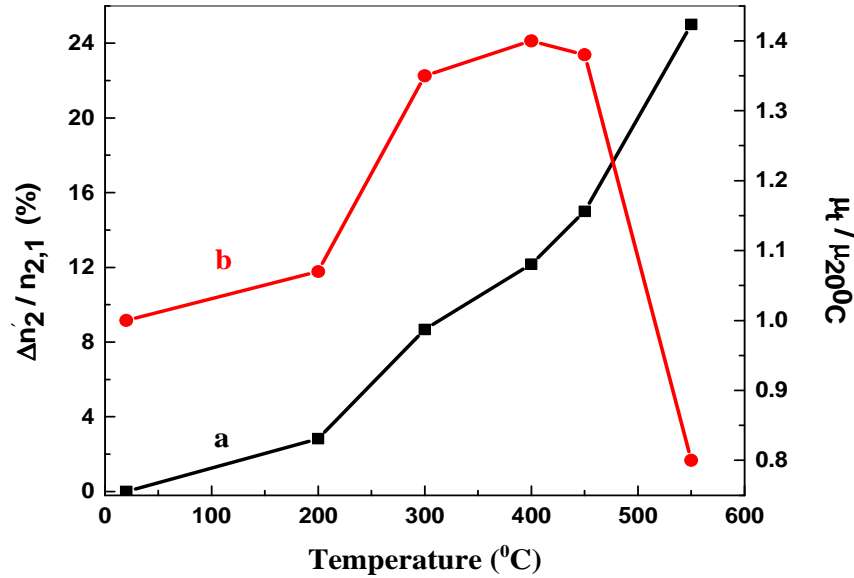


Figure 4. a) The annealing temperature dependence of the relative change in the electron state density near Fermi level, b) the dependence of the change in normalized magnetic permeability over the annealing temperature AMA $\text{Fe}_{73,5}\text{Cu}_1\text{Nb}_3\text{Si}_{15,5}\text{B}_7$.

The analysis of the experimental results represented in Fig. 4 and Fig. 1 shows that the temperature range from 20°C to 550°C, in which the structural changes were investigated, can be divided in several temperature subintervals.

Fig. 4 shows that the relative change in electron state density and the change in normalized magnetic permeability of the alloy annealed at 200°C, as compared to the as-cast sample, is relatively small being: $\frac{\Delta n_{2,200^\circ\text{C}-20^\circ\text{C}}}{n_{2,20^\circ\text{C}}} = 2,83\%$ and $\frac{\mu_{200^\circ\text{C}-20^\circ\text{C}}}{\mu_{20^\circ\text{C}}} = 7\%$. Small values of

these changes imply that the annealing of the as-cast sample of the amorphous alloy $\text{Fe}_{73,5}\text{Cu}_1\text{Nb}_3\text{Si}_{15,5}\text{B}_7$ does not lead to the significant structural changes in the alloy. Within the temperature range from 20°C to 200°C, the thermal energy is insufficient to transfer the atoms from the higher energy levels to the lower more stable levels. The annealing of the alloy at 300°C leads to a significant change in electron state density near Fermi level and in the normalized value of the magnetic permeability (Fig. 4): $\frac{\Delta n_{2,300^\circ\text{C}-20^\circ\text{C}}}{n_{2,20^\circ\text{C}}} = 8,67\%$ and $\frac{\mu_{300^\circ\text{C}-20^\circ\text{C}}}{\mu_{20^\circ\text{C}}} = 35\%$. Such big

changes imply that during the annealing at 300°C, an intensive process of structural relaxation occurs in the alloy. Upon the annealing at 400°C a relative change in the electron state density near Fermi level and the change in normalized magnetic permeability as compared to the alloy annealed at 300°C were only: $\frac{\Delta n_{2,400^\circ\text{C}-300^\circ\text{C}}}{n_{2,20^\circ\text{C}}} = 3,5\%$ and $\frac{\mu_{400^\circ\text{C}-300^\circ\text{C}}}{\mu_{20^\circ\text{C}}} = 5\%$. These results show

that during the heating from 300°C to 400°C, the structural relaxation occurs in the alloy at a far lesser extent. With the annealing of the alloy at 450°C and 550°C, the electron state density significantly increases near Fermi level, whereas the normalized value of magnetic permeability

considerably decreases: $\frac{\Delta n_{2,550^{\circ}\text{C}-450^{\circ}\text{C}}}{n_{2,20^{\circ}\text{C}}} = 10\%$ and $\frac{\mu_{550^{\circ}\text{C}-450^{\circ}\text{C}}}{\mu_{20^{\circ}\text{C}}} = -60\%$. The

significant increase in the electron state density and sudden decline in magnetic permeability in the temperature range from 450°C to 550°C is the consequence in the first place of nucleation and then of the crystallization of the amorphous phase in the alloy (Fig. 4).

Fig. 2 shows that upon the annealing of the alloy at 550°C, with the new heating the Curie temperature of the alloy exceeds 600°C. This confirms that during the annealing of the alloy at 550°C, the crystallization of the amorphous phase occurred in the alloy. The annealing of the alloy at 600°C does not cause significant changes in the electron state density near Fermi level and in the normalized magnetic permeability. These results show that the annealing of the alloy at 550°C can lead to a complete thermal stability of its structure.

The presented experimental results and their analysis show that on the basis of the temperature dependence of TEMF and magnetic permeability, the temperature intervals in which the structural relaxation and crystallization processes may be determined. In addition, it has been determined that there is a distinctive correlation between the structural changes, electron state density near Fermi level and magnetic permeability.

CONCLUSION

During the multiple annealings of the amorphous alloy sample $\text{Fe}_{73.5}\text{Cu}_1\text{Nb}_3\text{Si}_{15.5}\text{B}_7$ within the temperature range from 20°C to 600°C, the structural transformations occur in the alloy causing irretrievable changes in TEMF of thermocouple AMA – Cu and magnetic permeability of the alloy. During the heating of the as-cast sample to 200°C, structural changes occur in the alloy causing very small changes in the electron state density near Fermi level and in the magnetic permeability.

Within the temperature interval from 200°C to 300°C, an intensive structural relaxation occurs in the alloy. The amorphous structure of the alloy becomes orderly for a short, accompanied by simultaneous decrease in internal microstrains and the density of chaotically positioned dislocations, which leads to the increase in the electron state density near Fermi level and in the magnetic permeability. Within the temperature interval from 300°C to 400°C, the structural relaxation occurs to a much lesser extent. In that regard, the changes in electron state density and magnetic permeability are proportionally considerably smaller. Structural relaxation of about smaller intensity occurs in the temperature range from 400°C to 450°C. At the temperatures higher than 400°C, the stabilization of larger atoms and those more difficult to move Nb and Cu starts. These irretrievable structural changes cause increase in electron state density near Fermi level, yet smaller decline in magnetic permeability. In the temperature range from 450°C to 550°C, the nucleation processes occur, followed by crystallization of amorphous phase of the alloy. These processes cause sudden increase in the electron state density near Fermi level for about 15% and a sudden decline in normalized magnetic permeability of the cooled sample for about 60% as compared to the maximum permeability of the relaxed amorphous structure of the alloy.

Acknowledgements

The investigation was partially supported by the Ministry of Education, Science and Technological Development of the Republic of Serbia, under the following Project 172057.

References:

- [1] BERNAL, J.D. (1960): Geometry of the Structure of Monatomic Liquids. *Nature* **185**: 68-70.
- [2] HENDERSON, D.W. (1979): Thermal analysis of non-isothermal crystallization kinetics in glass forming liquids. *J. Non-Crystal. Solids* **30** (3): 301-315.
- [3] JONG, D.S., KIM, J.H., FLEURY, E., KIM, W.T., KIM, D.H. (2005): Synthesis of ferromagnetic Fe-based bulk glassy alloys in the Fe–Nb–B–Y system. *J. Alloys Compd.* **389** (1-2): 159-164.
- [4] KALEZIĆ-GLIŠOVIĆ, A. (2012): The structural relaxation effect on functional properties of Fe-based amorphous alloys. *PhD thesis*, Faculty of Physics, Belgrade. [in Serbian]
- [5] MARIČIĆ, A., SPASOJEVIĆ, M., ARNAUT, S., MINIĆ, D., RISTIĆ, M.M. (2008): The Effect of Structural Changes on Magnetic Permeability of Amorphous Powder Ni₈₀Co₂₀. *Sci. Sintering* **40**: 303-309.
- [6] MARIČIĆ, A., MINIĆ, D.M., BLAGOJEVIĆ, V.A., KALEZIĆ-GLIŠOVIĆ, A., MINIĆ, D.M. (2012): Effect of structural transformations preceding crystallization on functional properties of Fe_{73.5}Cu₁Nb₃Si_{15.5}B₇ amorphous alloy. *Intermetallics* **21** (1): 45-49.
- [7] MATUSITA, K., SAKKA, S. (1980): Kinetic study of crystallization of glass by differential thermal analysis—criterion on application of Kissinger plot. *J. Non-Crystal. Solids* **38** (39): 741-746.
- [8] MINIĆ, D.M., GAVRILOVIĆ, A., ANGERER, P., MINIĆ, D.G., MARIČIĆ, A. (2009a): Structural transformations of Fe₇₅Ni₂Si₈B₁₃C₂ amorphous alloy induced by thermal treatment. *J. Alloys Compd.* **476** (1-2): 705-709.
- [9] MINIĆ, D.M., MARIČIĆ, A., ADNAĐEVIĆ, B. (2009b): Crystallization of α -Fe phase in amorphous Fe₈₁B₁₃Si₄C₂ alloy. *J. Alloys Compd.* **473** (1-2): 363-367.
- [10] MINIĆ, D.M., MINIĆ, D.G., MARIČIĆ, A. (2009c): Stability and crystallization of Fe₈₁B₁₃Si₄C₂ amorphous alloy. *J. Non-Crystal. Solids* **355** (50-51): 2503-2507.
- [11] RAVAL, K.G., LAD, K.N., PRATAP, A., AWASTHI, A.M., BHARDWAJ, S. (2005): Crystallization kinetics of a multicomponent Fe-based amorphous alloy using modulated differential scanning calorimetry. *Thermochimica Acta* **425** (1-2): 47-57.
- [12] RIBIĆ-ZELENOVIĆ, L., RAFAILOVIĆ, L., SPASOJEVIĆ, M., MARIČIĆ, A. (2008): Correlation between electron state density change and the electrical resistivity and magnetic permeability changes in the nanostructured powder of the NiMo alloy. *Physica. B - Condensed Matter* **403** (12): 2148-2154.
- [13] SANTOS, D.R., SANTOS, D.S. (2001): Crystallization Kinetics of Fe-B Based Amorphous Alloys Studied in-situ using X-rays Diffraction and Differential Scanning Calorimetry. *Materials Research* **4** (1): 47-51.
- [14] TAKAYAMA, S. (1976): Amorphous structures and their formation and stability. *J. Mater. Sci.* **11** (1): 164-185.